Joint Inversion of Rayleigh Wave Phase Dispersion and Ellipticity and Receiver Functions for crustal S-wave velocity structure of Northern Taiwan

S55C-0127

Cheng, Yun-Ze[1], Hsin-Hua Huang[1,2], Fan-Chi Lin[3], Yu-Chien Lin[4], Wei-Chen Chen[5], Cheng-Nan Liu[3], Min-Hung Shih[6], and Cheng-Horng Lin[1]

1 Institute of Earth Sciences, Academia Sinica, Taipei 115, Taiwan 2 Department of Geosciences, National Taiwan University, Taiwan 3 Department of Geology and Geophysics, University of Utah, U.S.A. 4 Department of Earth and Life Science, University of Taipei, Taiwan
5 Department of Earth and Environmental Sciences, National Chung Cheng University, Taiwan6 National Center for Research on Earthquake Engineering, Taiwan

Introduction

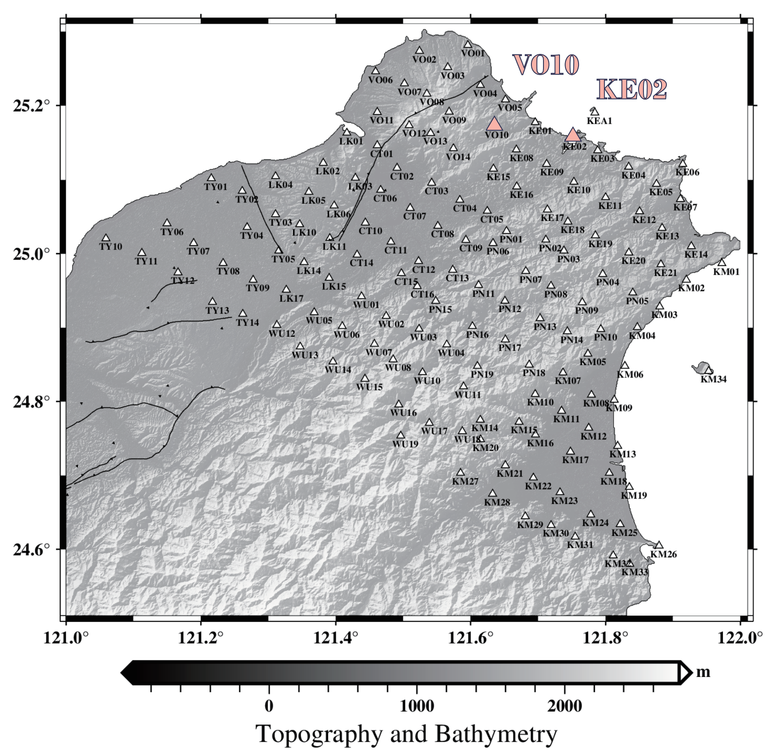

Figure 1. Formosa Array brodband stations distribution.
Black triangles indicate total 149 seismographs deployed in the northern Taiwan with spacing ~5km.

- Previous studies show the magma reservoir beneath Tatun volcanic plumbing system develop at 8-20km with significant P-wave velocity reduction (Huang et al., 2021).

- The detailed shallow crustal S-wave velocity structure (<10km) has been resolved via joint inversion of the noise-based Rayleigh wave phase velocity and ellipticity (Liu et al., 2021).

The deeper S-wave velocity property is crucial for understanding the magma chamber. However, the S-wave velocity properties of the magma reservoir are yet well constrained due to the short periods of noise correlation data (2-13 s).

Thus, to better constrain the Vs properties in the mid-to-lower crust, we conduct Markov Chain Monte Carlo (MCMC) joint inversion with
- Receiver function,
- Horizontal-to-vertical (H/V) amplitude ratio,
- Phase velocity

from noise cross-correlation function & telesiesmic events.
(2-13s) (14-50s).

Data

Set1: Rayleigh-wave measurements

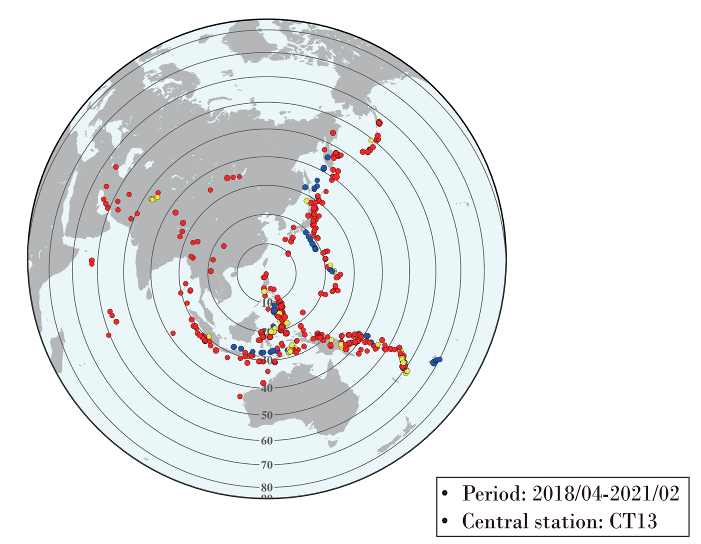

Figure 2. Locations of seismic events (circles) used in this study.
Red color denote events occured in depth 0-100km, yellow for 100-300km and blue for event depth larger than 300km.
Total 481 events with Mww>5.5 and Epicentraldistance 5-90 degrees.

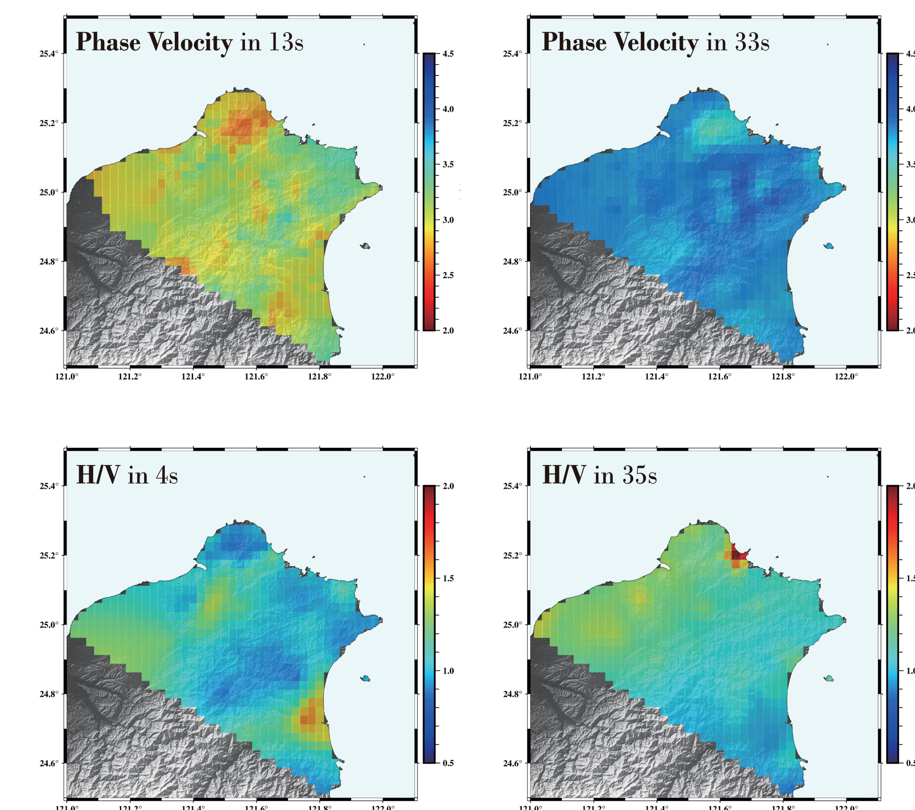

Figure 3. Interpolated Rayleigh wave H/V ratio and Phase velocity maps.
(a) Phase velocity maps at 13s. (b) Phase velocity at 33s.
(c) H/V ratio maps at 4s. (d) H/V ratio maps at 35s.

Set2: Receiver Functions

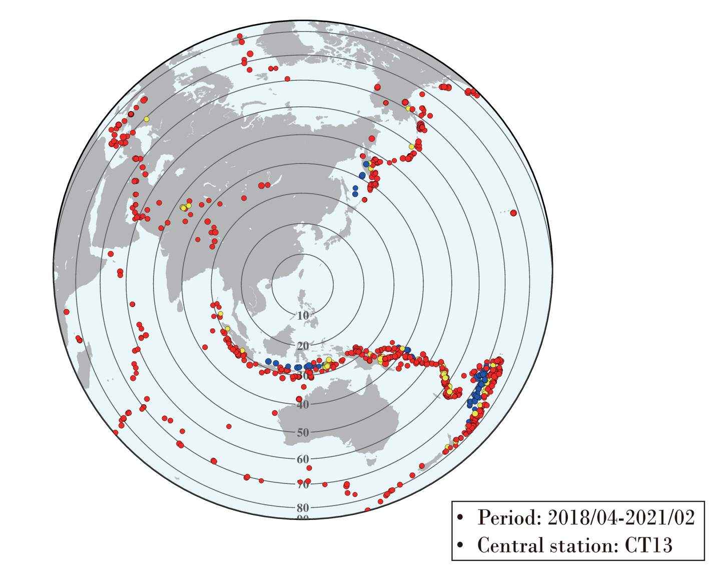

Figure 4. Distribution of teleseismic events and Stacking-RFs.
Same as Fig. 3. but with epicentral distance 30-90 degrees.

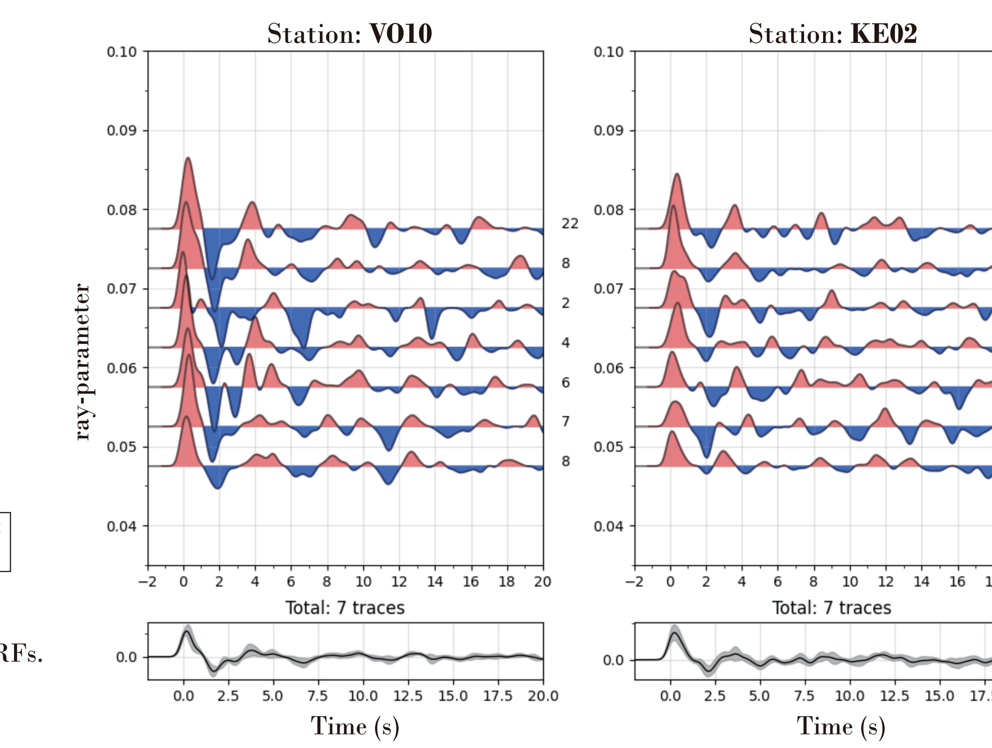

Figure5. Stacking-RF from stations near Tatun volcano group.
Receiver functions that have high signal-to-noise ratio from different ray-parameters (upper penals), and corresponding stacking-RF (lower panels).

Methods

Frequency-time analysis (FTAN):
Obtaining phase velocity dispersion curves. (Lin et al., 2008).

↓

Horizontal-to-vertical (H/V) ratio:
Process follow Lin et al. (2014) and Berg et al. (2018).

↓

Ekional tomography:
Phase velocity calculation follow Lin et al. (2009).

↓

Iterative deconvolution:
Receiver function computation (Ammon et al., 1991).

↓

Markov Chain Monte Carlo joint inversion:
Inversion procedure described in Berg et al. (2018).

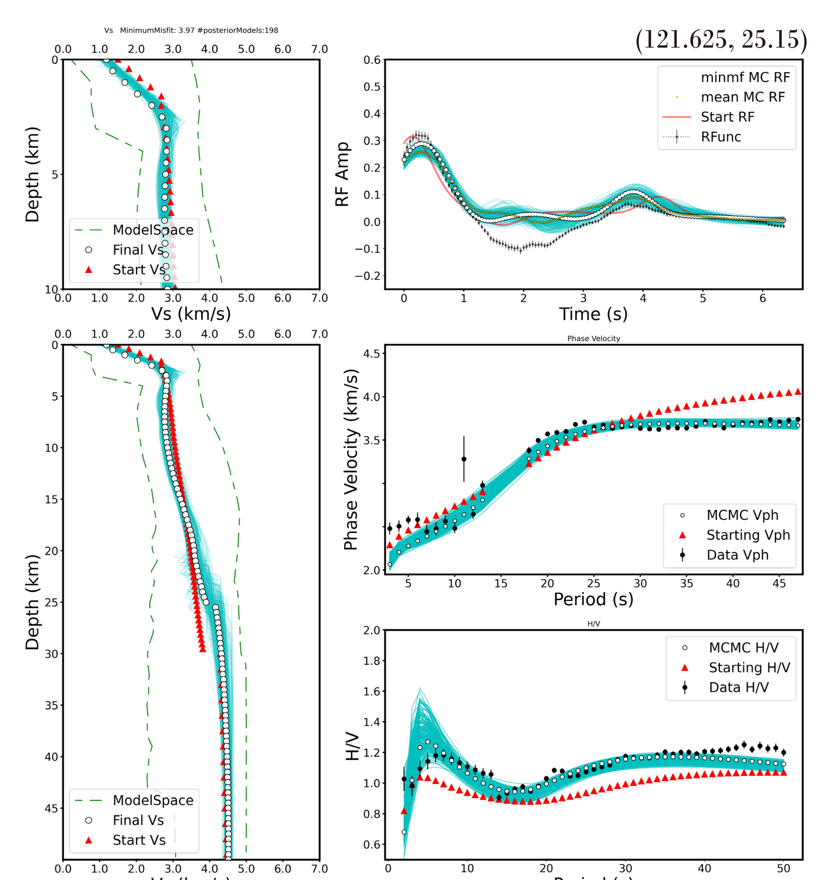

Figure 6. Example of 1-D MCMC joint inversion result with input data: Receiver function, Phase velocity, and H/V ratio.
(a) The inverted 1-D Vs profile in shallow depth (0-10km) (b) Same as (a) but extend to 50 km depth with the full searching space (green dash lines), starting model (red triangles), posterior models (cyan lines), and final 1-D model (white circles) identified. (c) The observed stacking receiver function with uncertainity (black dots and lines) and the receiver function predicted from the starting model (red triangles), posterior models (cyan lines). (d) and (e) Same as (c) but for phase velocity and H/V ratios .

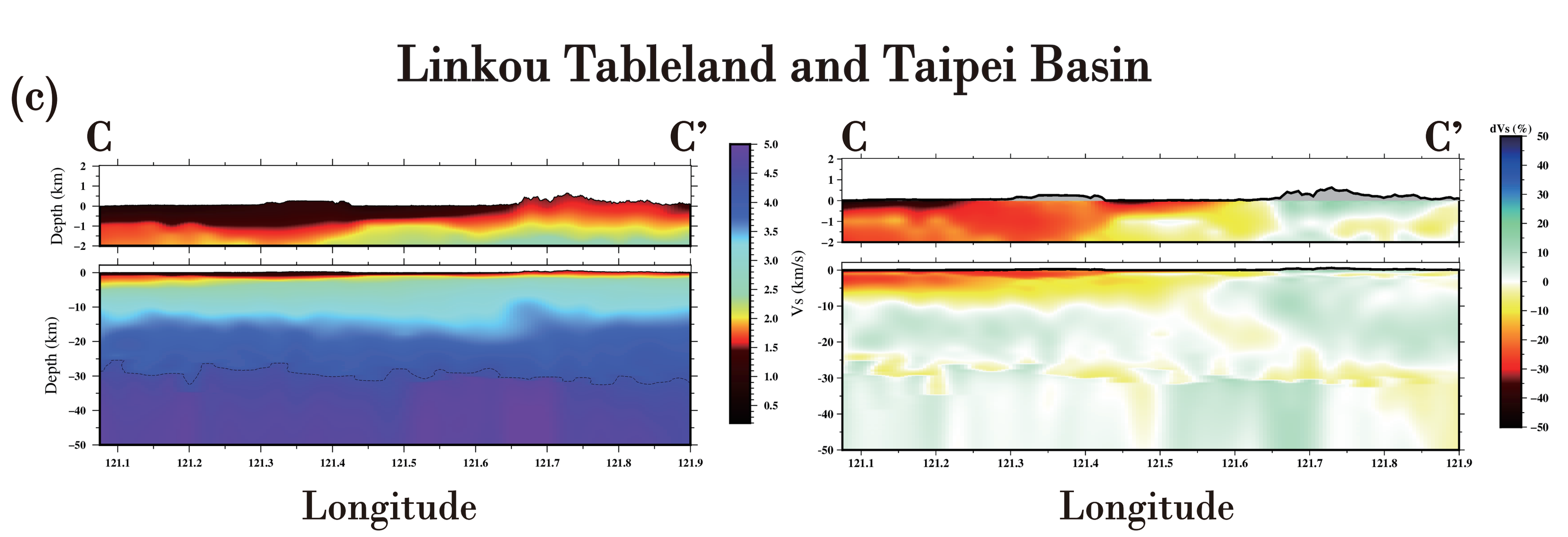

Results & Conclusions

1. The boundaries of velocity contrast (Low-velocity zone & Moho) are detected by receiver functions.
2. The new model revealed more details of mid-to-lower crustal structure after joint inverting Rayleigh wave measurements and receiver functions.
3. The depth range of the magma reservoir (5-15km) matches with Huang et al. (2021) P-wave tomography results (8-20km) but shows a wider geometry (sunny-side-up egg shape).
4. The low-velocity anomalies beneath Ilan plain may imply potential heat sources for geothermal exploration

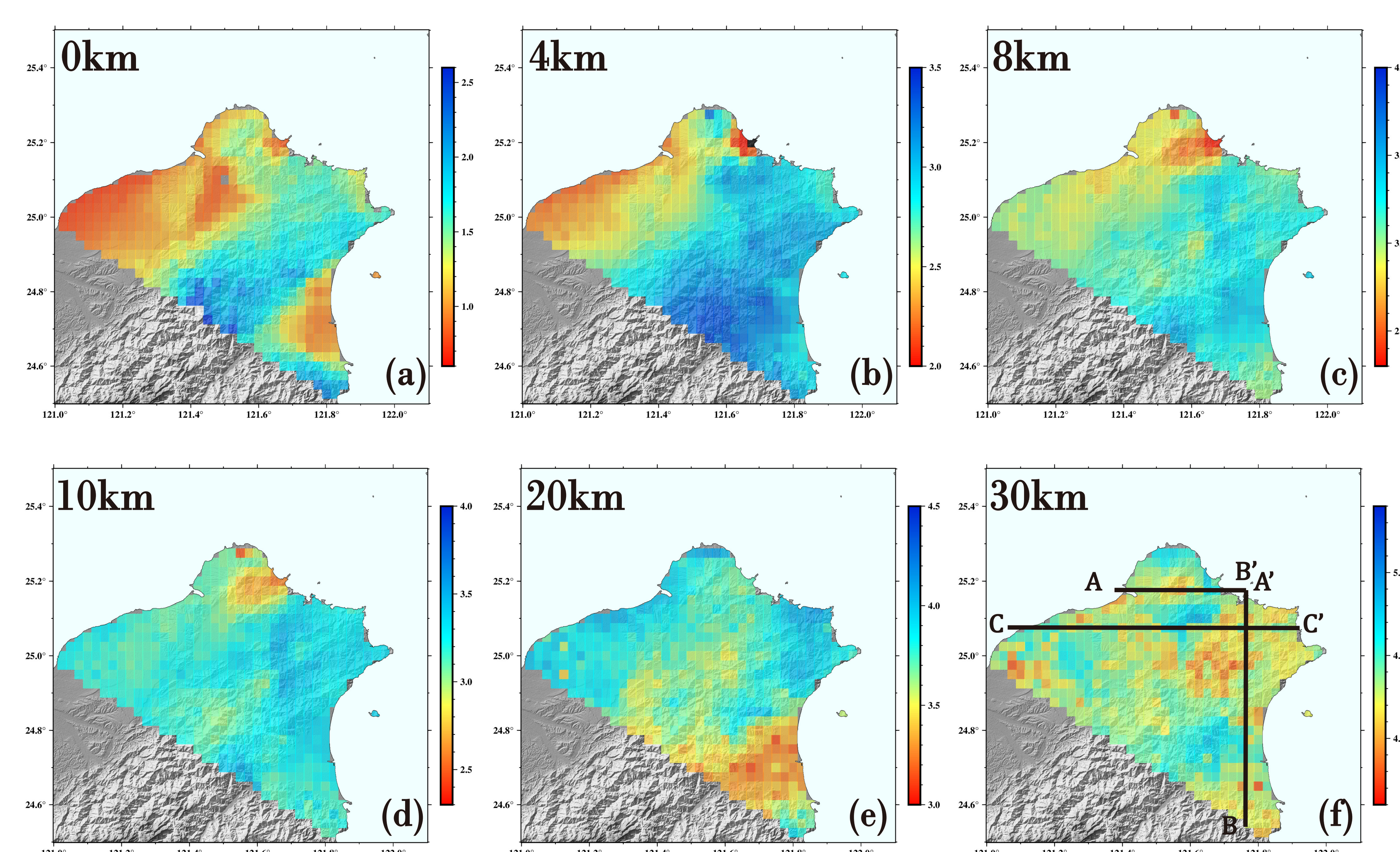

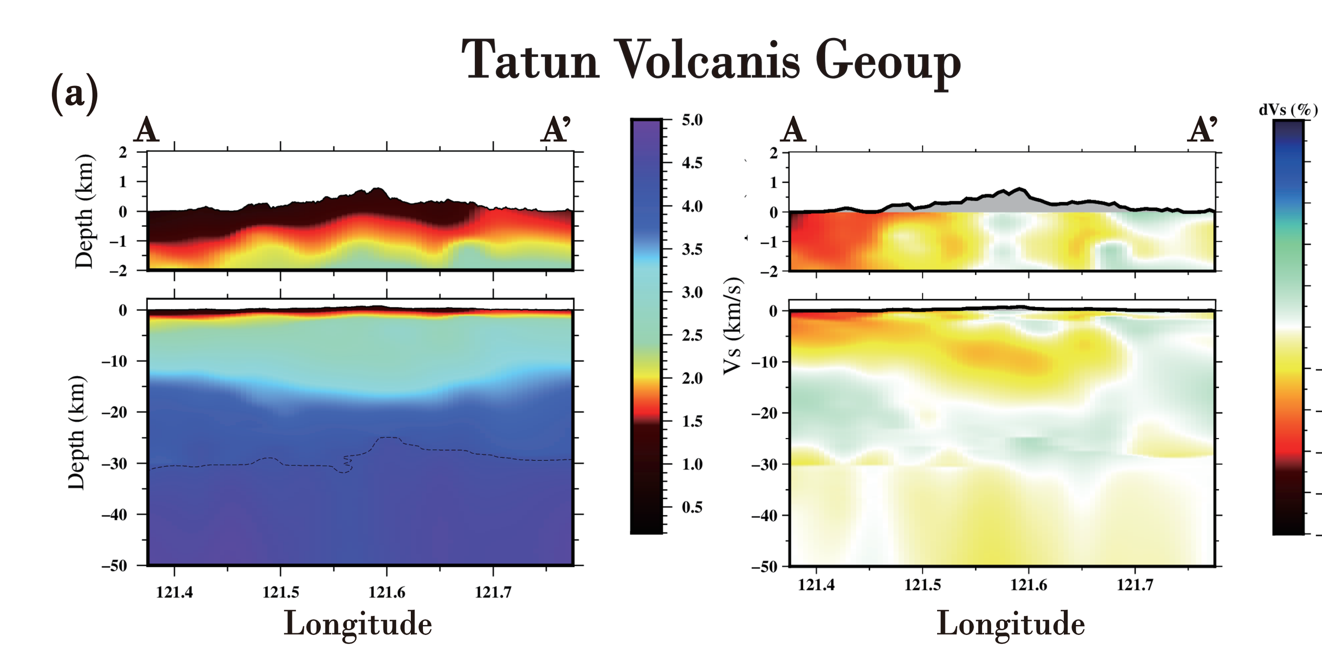

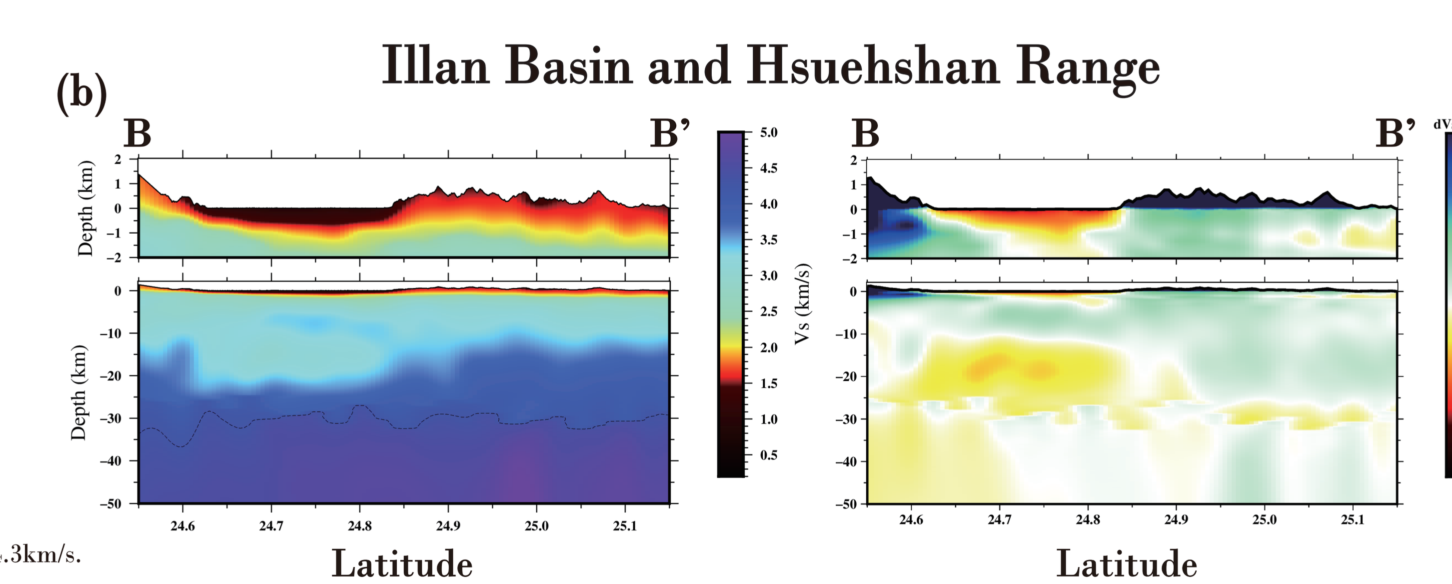

Figure 7. The final inverted S-wave velocity model. Red color denotes higher S-wave velocity (Vs). Depth slice at (a) 0km, (b) 4km, (c) 8km, (d) 10km, (e) 20km, and (f) 30km.
Figure 8. The specific cross sections along A-A', B-B', and C-C' profiles. The left figure is absolute values and the right is velocity perturbations. Dashed line denote the velocity equal to 4.3km/s.